

# Molecular Structure, Vibrational Spectroscopic (FT-IR, FT-Raman), UV and NLO Analysis of N-Methylurea by Density Functional Method

Loiusa Mary<sup>1,\*</sup>, D. Prem Anand<sup>2</sup>, A. Caroll Xavier<sup>3</sup>, L. Antony Selvam<sup>4</sup>

<sup>1</sup>Department of Computer Science, Sadakathullah Appa College, Tirunelveli, Tamil Nadu, India.

<sup>2,3,4</sup>Department of Physics, St. Xavier's College, Affiliated to Manonmaniam Sundaranar University, Palayamkottai, Tamil Nadu, India.

louisaselvakumar@gmail.com<sup>1</sup>, dpremanand@yahoo.co.in<sup>2</sup>, carollxavier21514@gmail.com<sup>3</sup>, profantony100@gmail.com<sup>4</sup>

**Abstract:** The theoretical investigations on the molecular structure and electronic and vibrational characteristics of n-methylurea are presented. DFT/B3LYP calculations obtained the vibration frequencies using a 6-31++G (d, p) basis set. The molecular equilibrium geometry of the title compound was fully optimized. Quantum chemical calculations of the equilibrium geometry were calculated with scaled quantum mechanics. Theoretically, the identification of atoms in molecular structure using IR spectrum in Gaussian software with 6-31++ (d, p) basis set. HOMO–LUMO energies, energy gap ( $\Delta E$ ), electro negativity ( $\chi$ ), chemical potential ( $\mu$ ), global hardness ( $\eta$ ), and softness (S) were calculated for the title molecule. The title compound has a low softness value (0.15517), and the calculated value of the electrophilicity index (2.29723) describes the biological activity. The stability and charge delocalization of the title molecule were studied by NLO behaviour in terms of first order polarizability; dipole moment and anisotropy of polarizability were accounted for the computed values of  $\mu$ ,  $\alpha$ , and  $\beta$  for the title molecule are 3.9248D,  $6.745026 \times 10^{-24}$  esu, and  $5.09515 \times 10^{-31}$  esu, respectively, which are greater than those of urea. High and non-zero  $\mu$  values suggest the chemical could be a promising NLO material. The title molecule's thermodynamic properties were examined at various temperatures, demonstrating relationships between heat capacity (Cp), entropy (S), and enthalpy changes ( $\Delta H$ ). The charges and variety are altered to reflect the different Mulliken charges for each case. We determine and assess adjacent reactivity descriptors based on electronic density.

**Keywords:** Non-Linear Optical (NLO); N-Methylurea Crystalline; Crystalline Hydrates; Entropy and Enthalpy; Anharmonic Corrections; Hyperpolarizability Values; Farthest Orbital; Low Electrophilicity; Organic Chemistry.

**Received on:** 27/01/2024, **Revised on:** 03/04/2024, **Accepted on:** 19/07/2024, **Published on:** 01/12/2024

**Journal Homepage:** <https://www.fmdbpub.com/user/journals/details/FTSASS>

**DOI:** <https://doi.org/10.69888/FTSASS.2024.000303>

**Cite as:** L. Mary, D. P. Anand, A. C. Xavier, and L. A. Selvam, “Molecular Structure, Vibrational Spectroscopic (FT-IR, FT-Raman), UV and NLO Analysis of N-Methylurea by Density Functional Method,” *FMDB Transactions on Sustainable Applied Sciences*, vol. 1, no. 2, pp. 54–63, 2024.

**Copyright** © 2024 L. Mary *et al.*, licensed to Fernando Martins De Bulhão (FMDB) Publishing Company. This is an open access article distributed under [CC BY-NC-SA 4.0](https://creativecommons.org/licenses/by-nc-sa/4.0/), which allows unlimited use, distribution, and reproduction in any medium with proper attribution.

## 1. Introduction

Urea and its derivatives are widely used and have a major impact on modern organic chemistry. Research on N-methylurea crystalline hydrates is detailed in this work. We used Fourier transform infrared spectroscopy and X-ray diffraction to look at

\*Corresponding author.

the original N-methylurea and its crystalline hydrates. The addition of water molecules to N-methylurea crystals causes a change in the location of the intensity peaks in the X-ray diffraction patterns and the FTIR spectra. Density functional theory at the B3LYP/6-31+G (d, p) level and atom-molecule theory has also been used to study gaseous methylurea crystalline hydrates [1]. Using the electron localization function and non-covalent reduced density gradient, the nature of hydrogen bond interactions between water and methyl-urea molecular contacts has been explored. The non-linear optical and thermodynamic characteristics of crystalline urea have been established. Hydrogen bond characteristics in methyl-urea crystalline hydrates have been studied using atomic-level computations, electron localization functions, and localized orbital locator topological studies. The molecular formula for n-methylurea is  $C_2H_6N_2O$ , and the molar mass is 74.08 g/mol (Figure 1).

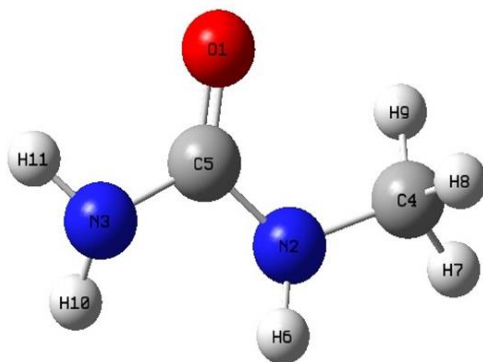


**Figure 1:** Structure of  $C_2H_6N_2O$  ( $E = -264.601280$  Hartree)

## 2. Techniques Employed

### 2.1. Computational details

The optimized  $C_2H_6N_2O$  structure, associated energies, and vibrational harmonic frequencies were computed by quantum chemical calculations and spectroscopic analysis with the use of the DFT (B3LYP) with a 6-31++G (d, p) basis set, all within the GAUSSIAN 16W software package. Using the stand and 6-31++G (d, p) basis set, the initial geometry was reduced without restriction on the potential energy surface at DFT, which was derived using standard geometrical parameters. We discovered the molecular properties, including the bond length and bond angle. For the molecule in question, many electronic parameters were computed, including HOMO, LUMO, energy gap, electro negativity, chemical potential, global hardness, and softness. Using the 6-311++G (d, p) basis set, the hyperpolarizability of the  $C_2H_6N_2O$  was also computed at the B3LYP level. We also calculated the  $C_2H_6N_2O$ 's non-linear optical characteristics, including its dipole moment and first-order hyperpolarizability. In order to find the thermodynamic variables, the online software THERMO was used. PL was used with a Gaussian 16W output. For the molecule in question, we created graphs showing the relationship between temperature and the thermodynamic variables entropy, specific heat capacity, and enthalpy.

## 3. Result and Discussion

### 3.1. Geometrical Properties

The advanced geometrical parameters for  $C_2H_6N_2O$  are resolved at the B3LYB level, and the premise set 6-31++G (d, p) is recorded and shown. These molecules have three N-C bonds, three C-H bonds, three N-H bonds, and one O-C bond. The average bond distances of N-C and N-H are 1.4095 Å and 1.0108 Å. The average bond distance of C-H is 1.0936 Å, and that of O-C is 1.2271 Å. The bond length N-C shows a higher value [2]. The bond between O-C-N has a higher value of 123.26°. The values of dihedral angles are selectively shown in Table 1. The planarity of the  $C_2H_6N_2O$  can be understood by comparing angle values between 0° and 180°.

**Table 1:** Optimized geometrical parameters of  $C_2H_6N_2O$ : bond length, bond angle, and dihedral angle

| Parameter      |                        | Parameter      |                        |
|----------------|------------------------|----------------|------------------------|
| Bond Length(Å) | B3LYP/6-31++<br>G(d,p) | Bond Angle (°) | B3LYP/6-31++<br>G(d,p) |
| O-C            | 1.2271                 | C-N-C          | 119.8086               |

|                          |                                |       |          |
|--------------------------|--------------------------------|-------|----------|
| N-C                      | 1.4573                         | C-N-H | 116.7469 |
| N-C                      | 1.3788                         | C-N-H | 116.9464 |
| N-H                      | 1.0105                         | C-N-H | 118.2909 |
| N-C                      | 1.3926                         | C-N-H | 112.8142 |
| N-H                      | 1.0112                         | H-N-H | 114.3589 |
| N-H                      | 1.0107                         | N-C-H | 108.9496 |
| C-H                      | 1.0927                         | N-C-H | 112.5204 |
| C-H                      | 1.0976                         | N-C-H | 108.8118 |
| C-H                      | 1.0906                         | H-C-H | 109.2824 |
| <b>Dihedral Angle(Å)</b> | <b>B3LYP/6-31++<br/>G(d,p)</b> | H-C-H | 109.1094 |
|                          |                                | H-C-H | 108.1133 |
| C-N-C-H                  | -163.134                       | O-C-N | 123.2676 |
| C-N-C-H                  | 75.512                         | O-C-N | 122.3091 |
| C-N-C-H                  | -44.2766                       | N-C-N | 114.4192 |
| H-N-C-H                  | 45.9913                        |       |          |
| H-N-C-H                  | -75.363                        |       |          |
| H-N-C-H                  | 164.8484                       |       |          |
| C-N-C-O                  | 8.0765                         |       |          |
| C-N-C-N                  | -171.199                       |       |          |
| H-N-C-O                  | 158.8952                       |       |          |
| H-N-C-N                  | -20.3802                       |       |          |
| H-N-C-O                  | 149.8391                       |       |          |
| H-N-C-N                  | -30.8777                       |       |          |
| H-N-C-O                  | 12.5685                        |       |          |
| H-N-C-N                  | -168.148                       |       |          |

### 3.2. Vibrational Spectral Analysis

It is theoretically possible to perform vibrational spectrum computations by modifying the density functional method B3LYP/6-31++G (d, 2p). Overestimation of vibrational frequencies by DFT potentials leads to anomalies that can be corrected by measuring anharmonic corrections with great precision [3]. The title molecule contains eleven atoms and exhibits twenty-seven fundamental vibrations characteristic of the C1 point group asymmetric molecule. Figure 6 displays the calculated infrared spectra of the compounds that were suggested. In aromatic compounds, the N-H bending occurs in the range of 1600-1580  $\text{cm}^{-1}$ , and the molecule has its bending in 1672  $\text{cm}^{-1}$  (Figure 3). The important one to consider is the C - Cl stretching, which is obtained in the 561  $\text{cm}^{-1}$  range of 850 - 550  $\text{cm}^{-1}$  (Figure 2).

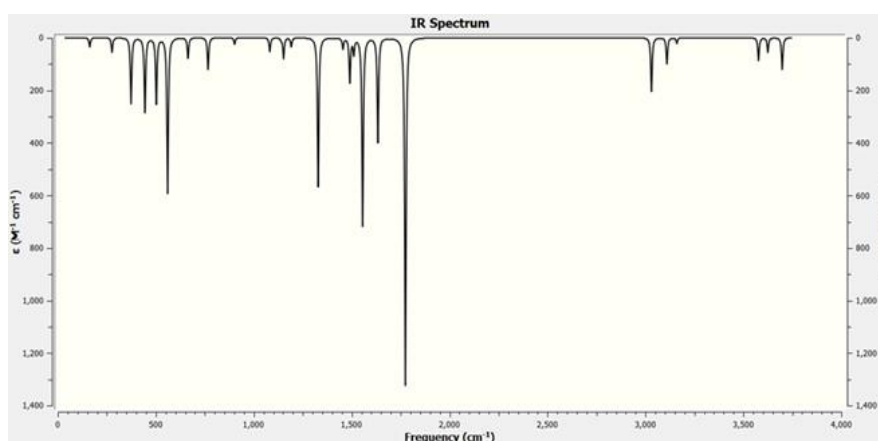
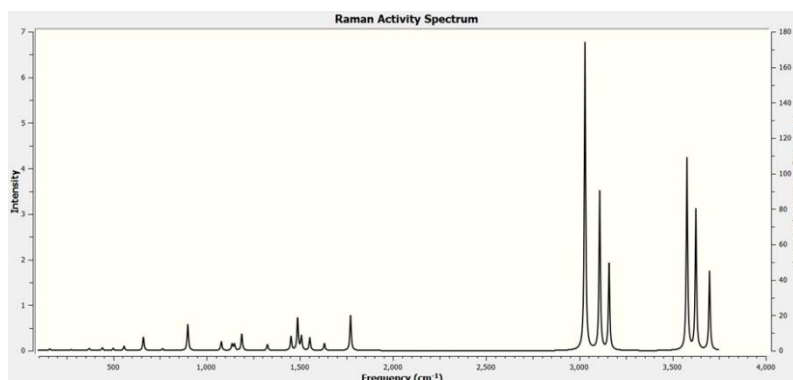


Figure 2: IR Spectrum of C<sub>2</sub>H<sub>6</sub>N<sub>2</sub>O



**Figure 3:** Raman spectrum of  $C_2H_6N_2O$

### 3.3. Non-Linear Optical (NLO) Properties

We used the density-functional theory (DFT) method to examine the NLO properties of a gas-phase isolated molecule of the title molecule, looking for signs of NLO character in its computed polarizability, hyperpolarizability, and dipole moment [4]. The hyperpolarizabilities are very sensitive to the basis sets used, and the theoretical approach used, which causes a change in the hyperpolarizability as a result of electron correlation. Organic compounds with N-H groups have improved molecular hyperpolarizability and mechanical stabilities as a result of hydrogen bond interaction [5]. In Table 2, you can see the predicted values.

The strong intermolecular contact is sufficiently indicated by the high dipole moment value of 3.9248 D. The optimized values' dipolar character is accurately depicted by the non-zero values of the dipole moment. Urea is a common starting point for comparison studies since it is a model molecule for investigating the NLO characteristics of molecular systems. The first-order hyperpolarizability ( $\beta$ ) value for the title molecule is calculated as  $5.09515 \times 10^{-31}$  esu, which is much larger than that of urea ( $0.3728 \times 10^{-30}$ ). According to the title molecule's high hyperpolarizability value, it possesses significant NLO characteristics [7]. Consequently, more research into the title molecule's NLO characteristics can be undertaken. This expansion turns into when the external electric field is weak and uniform.

$$E = E^0 - \mu_\alpha F_\alpha - 1/2(\alpha_{\alpha\beta} F_\alpha F_\beta) - 1/6(\beta_{\alpha\beta\gamma} F_\alpha F_\beta F_\gamma) \dots$$

Where  $E^0$  is the energy of the unperturbed atoms,  $F_\alpha$  is the field at the beginning,  $\mu_\alpha$  is the part of dipole moment,  $\beta$  is the segment to F polarizability, and  $\beta_{\alpha\beta\gamma}$  is the segment to F first hyperpolarizability [8]. The dipole moment ( $\mu$ ), the mean polarizability ( $\alpha_0$ ), the anisotropy of the polarizability ( $\Delta\alpha$ ), and the mean first hyperpolarizability ( $\beta_0$ ) utilizing x, y, z parts are characterized as:

$$\mu = (\mu_x^2 + \mu_y^2 + \mu_z^2)^{\frac{1}{2}}$$

$$\alpha_0 = (\alpha_{xx} + \alpha_{yy} + \alpha_{zz}) / 3$$

$$\Delta\alpha = 2 \frac{1}{2} (\alpha_{xx} + \alpha_{yy})^2 + (\alpha_{yy} + \alpha_{zz})^2 + (\alpha_{zz} + \alpha_{xx})^2 + 6 \alpha_{xx}^2)^{\frac{1}{2}}$$

$$\beta_0 = (\beta_x^2 + \beta_y^2 + \beta_z^2)^{\frac{1}{2}}$$

where,  $\beta_x = \beta_{xxx} + \beta_{xyy} + \beta_{xzz}$ ;  $\beta_y = \beta_{yyy} + \beta_{xxy} + \beta_{yzz}$ ;  $\beta_z = \beta_{zzz} + \beta_{xxz} + \beta_{yyz}$

### 3.4. Electrical Properties

The meaning of the Highest Occupied Molecular Orbital (HOMO) and the Lowest Unoccupied Molecular Orbital (LUMO) is of basic importance as it shapes the reason for thinking little of the substance strength and reactivity of the tile molecules. The HOMO can be considered as the farthest orbital-bearing electron that seems to spread these electrons as an electron given. In contrast, the LUMO can be considered the deepest orbital containing a free destination to accept electrons, portraying the sub-atomic weakness to nucleophilic assaults [9]. The energy distinction between the HOMO orbital and the LUMO is referred to

as the energy gap, which implies that the atom is more receptive with the least energy distinction among HOMO and LUMO. The bigger the dipole moment, the more noteworthy the intermolecular interactions. Grouping an atom as a hard and delicate particle dependent on substance hardness is considerable. The larger HOMO-LUMO energy gap uncovers that the tile molecule is a hard atom, and the little HOMO-LUMO energy gap shows that it is a delicate atom (Figure 4). The energy differences between HOMO and LUMO portray the possible collaborations of charge transfer inside the atom. On account of the collaboration between the compound orbital HOMO and LUMO, the transition condition of the double bond  $\pi$ - $\pi^*$  structure is found using the molecular orbital hypothesis [10]. The orbital includes the finesses of the electron density, which is then used to determine which component of the particle is usually correlated with the energy-transfer case. There is a one-to-one relationship between the HOMO energy and the ionization potential (IP) and between the LUMO energy and the electron affinity (EA) [11]. The ionization potential is characterized by the energy distinction between the energy of the compound produced from the electron transfer ( $E_{\text{cation}}$  - the energy of the extreme cation) and the particular nonpartisan compound ( $E_n$ ).

$$\text{IP} = E_{\text{cation}} - E_n; \text{IP} = - E_{\text{HOMO}}$$

The Electron affinity (EA) is resolved on the energy distinction between the nonpartisan atom ( $E_n$ ) and the anion particle  $E_{\text{anion}}$ .

$$\text{EA} = E_n - E_{\text{anion}}; \text{EA} = - E_{\text{LUMO}}$$

For the title entitled adapting B3LYP/6-311++G(d,p) base set, HOMO energy ( $E_{\text{HOMO}}$ ), LUMO energy ( $E_{\text{LUMO}}$ ), energy gap ( $\Delta E$ ), Electro negativity ( $\chi$ ), Chemical potential ( $\mu$ ), Global hardness ( $\eta$ ), and Softness (S) are determined. Both the HOMO and the LUMO are the major orbitals engaged with compound harmony [12]. The estimated HOMO and LUMO energy are listed.

$$\text{Electronegativity } (\chi) = -\frac{1}{2}(E_{\text{LUMO}} + E_{\text{HOMO}})$$

$$\text{Chemical potential } (\mu) = -\chi = \frac{1}{2}(E_{\text{LUMO}} + E_{\text{HOMO}})$$

$$\text{Global hardness } (\eta) = \frac{1}{2}(E_{\text{LUMO}} - E_{\text{HOMO}})$$

$$\text{Electrophilicity } (\omega) = \mu^2 / 2\eta$$

The inverse global hardness esteems are characterized as Softness (S), which is a particle's property that gauges the substance reactivity level.

$$\text{Global Softness } (S) = 1/2\eta$$

The effectiveness of this new reactivity level has been shown in recognizing the harmfulness of different contaminants in terms of their reactivity and site selectivity. The N-METHYLUREA compound has a low softness and low electrophilicity. It has a low energy gap.

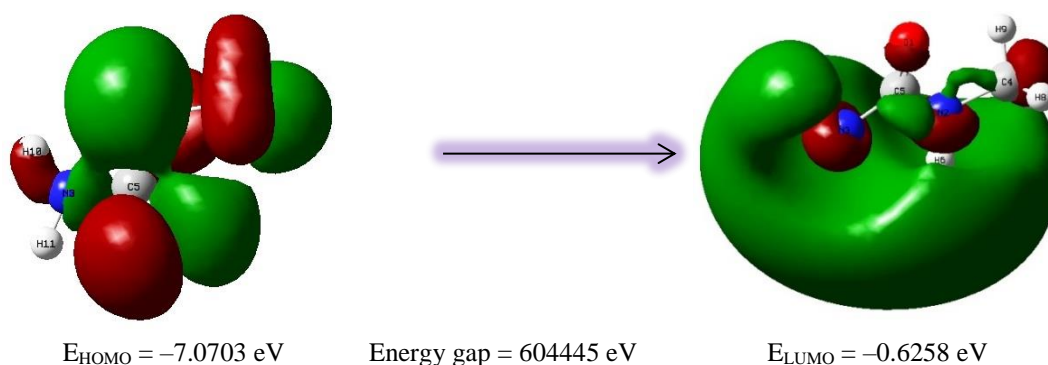


**Figure 4:** HOMO – LUMO structure

**Table 2:** The values of calculated first-order hyperpolarizability ( $\beta$ ), mean polarizability ( $\alpha$ ), and dipole moment ( $\mu$ ) of the title compound

| Parameter         | Hyperpolarizability of $C_2H_6N_2O$ | Parameter          | Polarizability and Dipole moment of $C_2H_6N_2O$ |
|-------------------|-------------------------------------|--------------------|--|
| $\beta_{xxx}$     | -12.2998                            | $\alpha_{xx}$      | -24.1062   |
| $\beta_{yyy}$     | -15.4413                            | $\alpha_{yy}$      | -32.1144   |
| $\beta_{zzz}$     | 0.0431                              | $\alpha_{zz}$      | -32.4224   |
| $\beta_{xyy}$     | 0.4302                              | $\alpha_{xy}$      | 1.7523   |
| $B_{xyy}$         | -1.3473                             | $\alpha_{xz}$      | 2.1749   |
| $\beta_{xxz}$     | -4.4864                             | $\alpha_{yz}$      | 0.2332   |
| $\beta_{zzz}$     | 0.8273                              | $\alpha_0$ (a.u)   | 45.513000  |
| $\beta_{yzz}$     | 1.6290                              | $\alpha_0$ (e.s.u) | $6.745026 \times 10^{-24}$                       |
| $\beta_{yyz}$     | -0.7954                             | $\mu_x$            | 0.2868   |
| $\beta_{xyz}$     | -3.0823                             | $\mu_y$            | -3.8958  |
| $\beta_0$ (a,u)   | 60.879073                           | $\mu_z$            | -0.3803  |
| $\beta_0$ (e.s.u) | $5.09515 \times 10^{-31}$           | $\mu_{total}$ (d)  | 3.9248   |

### 3.5. Thermal Properties

In solid-state science, the investigation of the thermodynamic properties of a compound is exceptionally huge. It is perceived as a significant component in the plan of reasonable items to be utilized under high temperatures and high pressing factors. The cumulative energy of an atom, i.e.,  $E = E_t + E_r + E_v + E_e$ , is the amount of translational, rotational, vibrational, and electronic energy. Considering the particle at a room temperature of 298.15 K and one atmospheric pressure, the statistical thermochemical study of the title compound is performed. Standard thermodynamic capacities depend on vibrational investigation and numerical thermodynamics (Figure 6). Specific heat capacity ( $C_p$ ), entropy (S), and enthalpy ( $\Delta H$ ) are obtained from theoretical harmonic frequencies utilizing the THERMO.PL program. The results are listed in Table 4. From the translational energy, the ascent in temperature from 100 K to 1000 K increases all the estimations of  $C_p$  and  $\Delta H$ , which is upheld by the expansions in the powers of sub-atomic vibration Table 3.

From the graph, we infer that the temperature rises when the  $C_p$ , S, and  $\Delta H$  estimations are equivalent to the temperature under constant pressure [13]. Since the disorder increments with thermal agitation, it influences the entropy of a framework with expanding temperature (Figure 8). The conduct of materials under different thermodynamic imperatives can be clarified regarding the specific heat of a solid (Figure 5). It additionally clarifies how the material stores heat energy proficiently (Figure 7). It is demonstrated that, with an improvement in temperature, the heat capability of the title compound increments effectively at a lower temperature range. The thermodynamic properties relationships are examined using quadratic formulae, and temperatures are fitted [14]. The correlation of temperature dependency fitting equations for n-methylurea is given by.

$$S = 232.6 + 17.105 T - 0.3137 T^2 \quad (R^2 = 0.9978)$$

$$C_p = 40.644 + 10.782 T + 40.644 T^2 \quad (R^2 = 0.998)$$

$$\Delta H = 2.2292 + 1.7871T + 2.2292 T^2 \quad (R^2 = 0.999)$$

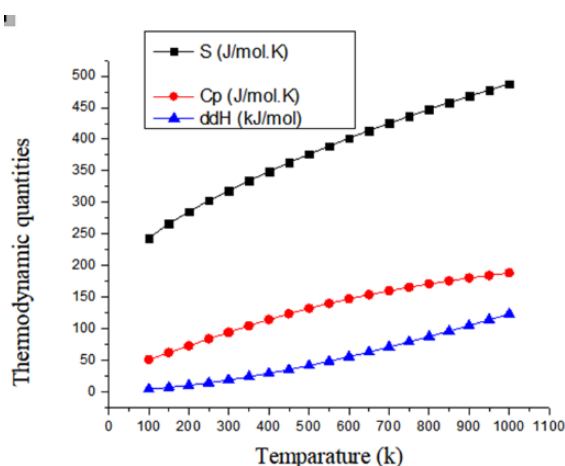


**Figure 5:** Graphical representation of Thermodynamic function

**Table 3:** Calculated the energy value of C<sub>2</sub>H<sub>6</sub>N<sub>2</sub>O

| Parameter                     | Value       |
|-------------------------------|-------------|
| HOMO (eV)                     | -7.07033408 |
| LUMO (eV)                     | -0.62586185 |
| Ionization Potential (IP)     | 7.07033408  |
| Electron Affinity (EA)        | 0.62586185  |
| Energy gap(eV)                | 6.444523228 |
| Chemical potential( $\mu$ )   | 3.84797     |
| Electro Negativity ( $\chi$ ) | -3.84797    |
| Chemical hardness ( $\eta$ )  | 3.22276     |
| Chemical softness (S)         | 0.15517     |
| Electrophilicity ( $\omega$ ) | 2.29723     |

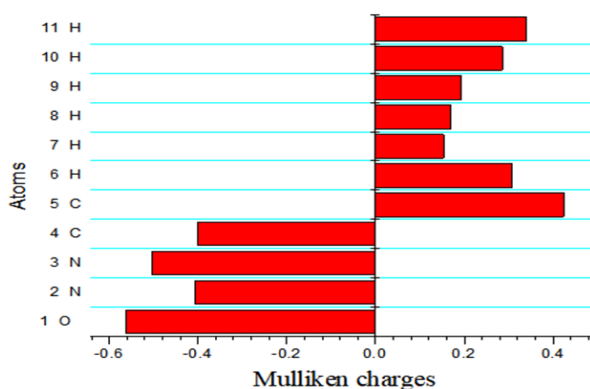


**Figure 6:** The Histogram of calculated Mulliken Charge of C<sub>2</sub>H<sub>6</sub>N<sub>2</sub>O

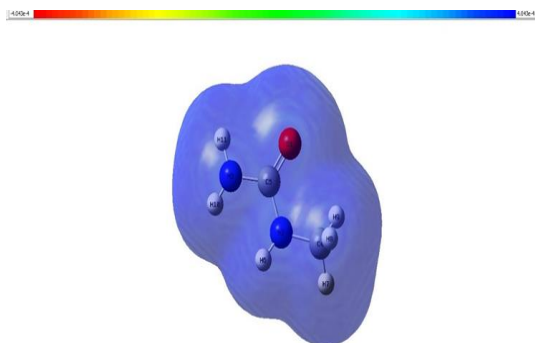


**Figure 7:** MEP of C<sub>2</sub>H<sub>6</sub>N<sub>2</sub>O

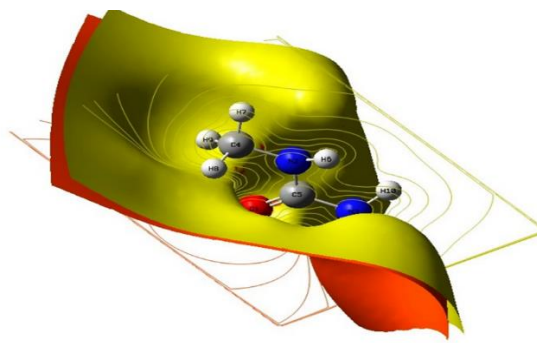


**Figure 8:** Contour of C<sub>2</sub>H<sub>6</sub>N<sub>2</sub>O

**Table 4:** Thermodynamic functions variation of C<sub>2</sub>H<sub>6</sub>N<sub>2</sub>O

| T (K)  | Heat capacity(S) (J/mol.K) | Entropy (Cp) (J/mol.K) | Enthalpy ( $\Delta H$ ) (kJ/mol) |
|--------|----------------------------|------------------------|----------------------------------|
| 100    | 243.433                    | 50.78                  | 4.051                            |
| 150    | 266.096                    | 61.82                  | 6.865                            |
| 200    | 285.394                    | 72.819                 | 10.232                           |
| 250    | 302.798                    | 83.527                 | 14.142                           |
| 298.15 | 318.379                    | 93.659                 | 18.408                           |
| 300    | 318.959                    | 94.044                 | 18.582                           |
| 350    | 334.232                    | 104.312                | 23.542                           |
| 400    | 348.809                    | 114.155                | 29.006                           |
| 450    | 362.795                    | 123.411                | 34.948                           |

|      |         |         |         |
|------|---------|---------|---------|
| 500  | 376.248 | 131.994 | 41.336  |
| 550  | 389.204 | 139.888 | 48.136  |
| 600  | 401.691 | 147.125 | 55.314  |
| 650  | 413.733 | 153.764 | 62.838  |
| 700  | 425.355 | 159.867 | 70.681  |
| 750  | 436.579 | 165.494 | 78.817  |
| 800  | 447.428 | 170.701 | 87.223  |
| 850  | 457.923 | 175.532 | 95.881  |
| 900  | 468.085 | 180.026 | 104.771 |
| 950  | 477.932 | 184.215 | 113.878 |
| 1000 | 487.482 | 188.126 | 123.188 |

### 3.6. Mulliken Charge Analysis

Using the Mulliken atomic charge analysis method, the distribution of charges for N-methyl urea was determined. A molecular's positive and negative charge distribution determines the majority of the variation in bond lengths between different atoms. Fifth Table. Chemical calculations in a molecular system rely heavily on atomic calculations because of the importance of atomic charges, dipole moment, molecular polarizability, electronic structure, acidity basic behaviour, and other molecular features [6]. Table 6 displays the values of the charges for the atoms in the title chemical as measured using the B3LYP functional Mulliken population analysis (MPA) method. To ensure the validity of the results, the study necessitates the participation of an adult with adolescent children. With 294 married and 290 single, the sample does not exhibit a significant bias in terms of marital status. According to Table 1, the demographic profile indicates that the study's respondents are legitimate and provide some credible responses.

**Table 5:** Thermodynamic Parameters of C<sub>2</sub>H<sub>6</sub>N<sub>2</sub>O

| Structural Parameters  | Thermodynamic Parameters of C <sub>2</sub> H <sub>6</sub> N <sub>2</sub> O |
|--|--|
| SCF Energy (Hartree)   | -264.601280  |
| Total Energy(thermal), E <sub>total</sub> (kcal.mol <sup>-1</sup> )    | 61.345   |
| Heat Capacity C <sub>v</sub> (cal.mol <sup>-1</sup> .k <sup>-1</sup> ) | 20.398   |
| Entropy S (cal.mol <sup>-1</sup> .k <sup>-1</sup> )                    | 76.068   |
| Rotational Constants (GHz)   |  |
| A  | 10.42204   |
| B  | 4.02673  |
| C  | 2.97184  |

**Table 6:** Mulliken charges of C<sub>2</sub>H<sub>6</sub>N<sub>2</sub>O

| Atoms | Mulliken Charges |
|-------|------------------|
| 1 O   | -0.562009        |
| 2 N   | -0.407727        |
| 3 N   | -0.504259        |
| 4 C   | -0.401139        |
| 5 C   | 0.424016         |
| 6 H   | 0.307107         |
| 7 H   | 0.153569         |
| 8 H   | 0.170337         |
| 9 H   | 0.193906         |
| 10 H  | 0.285353         |
| 11 H  | 0.340847         |

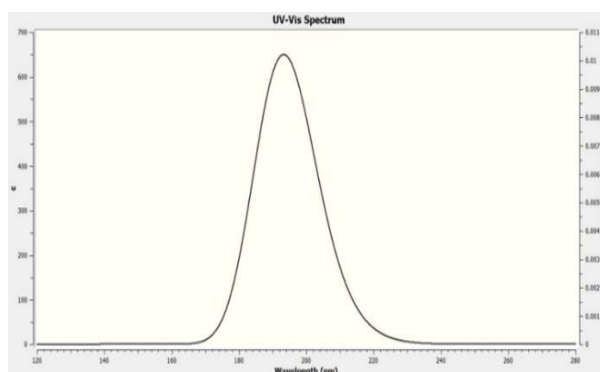
### 3.7. UV Spectrum

Figure 7 displays the UV-Vis absorption spectra acquired using the DMSO solvent. The experimental results are in good agreement with the theoretical predictions, as can be shown in Table 7. At 207 nm, with an oscillation strength of 0.0009, a very good maximum peak is found. At 2195 and 2189 nm, you can see the additional peaks. The TD-DFT/CAM-B3LYP

method and the 6-31++G(d,p) basis set, with DMSO as the solvent, are used to compute the values. The band gap of the opposite functional group was similarly calculated theoretically with the same basis set. The electron's excitement as it moves from a lower to an upper level, as well as the effect of various functional groups, causes the fluctuation. Figure 9 shows that while frequency and energy rise, the absorption wavelength decreases.

**Table 7:** Theoretical electronic absorption spectra values of title compound using TD-DFT/B3LYP/6-31+G (d,p) basis set

| Excited State | Wavelength $\lambda$ (nm) | Excitation energies(eV) | Oscillator Strengths (f) |
|---------------|---------------------------|-------------------------|--------------------------|
| S1            | 207.65                    | 5.9707                  | 0.0009                   |
| S2            | 194.95                    | 6.3598                  | 0.0108                   |
| S3            | 189.28                    | 6.5502                  | 0.0058                   |



**Figure 9:** UV Spectrum of  $C_2H_6N_2O$

#### 4. Conclusion

Using a B3LYP/6-31++G (d, p) basis set, the vibrational analysis of the n-methylurea was conducted using density-functional theory methodology. In order to calculate the other parameters for this study, the geometric parameters (bond angle, bond length) were first calculated. Elements' presence and structural determination can be ascertained using vibrational analysis. The title chemical exhibited higher computed hyperpolarizability values when urea was used as a model NLO material. This raises the prospect that the chemical in the title could be NLO active. The fact that this derivative of piperazine is bioactive suggests that the compound under research has high levels of biological activity, chemical softness, and chemical hardness, according to the results of frontier molecular analysis. The title molecule has calculated values of  $\mu$ ,  $\alpha$ , and  $\beta$  that are higher than urea. Based on these findings, the title chemical could be a promising NLO candidate. With a high electrophilicity index of 0.25995, it is also a significant class of compounds in medicinal chemistry. As the temperature rises, thermal gradients such as Cp, S, and  $\Delta H$  get larger, which is because the molecular vibrations become stronger. This study compares the change in the Mulliken charges in each example by varying the charges and multiplicity.

**Acknowledgment:** The authors would like to express their sincere gratitude to Sadakathullah Appa College and St. Xavier's College for their invaluable support and encouragement. Their contributions were instrumental in the successful completion of this work.

**Data Availability Statement:** Data supporting the findings of this study are available from the corresponding authors upon reasonable request.

**Funding Statement:** This research was conducted, and the manuscript was prepared without any external financial assistance or funding.

**Conflicts of Interest Statement:** The authors declare that there are no conflicts of interest related to this work.

**Ethics and Consent Statement:** Ethical standards were followed in this study, with informed consent obtained from all participants and strict confidentiality maintained throughout.

## References

1. G. Kang, T. H. Kim, E.-J. Lee, and C. H. Kang, "Crystal structure of 2-bromo-4,6-dinitroaniline," *Acta Crystallogr. Sect. E Struct. Rep. Online*, vol. 71, no. 11, p. 813, 2015.
2. M. Gnanaprakasam, G. Saranya, S. Bandaru, K. Senthikumar, and N. J. English, "Atmospheric oxidation mechanism and kinetics of 2-bromo-4,6-dinitroaniline," *Phys. Chem. Chem. Phys.*, vol. 21, no. 12, pp. 21109–21127, 2019.
3. X. Xie, Y. Jin, Z. Ma, S. Tang, H. Peng, J. P. Giesy, and H. Liu, "Underlying mechanism of reproductive toxicity caused by multigenerational exposure of 2-bromo-4,6-dinitroaniline to zebrafish at environmental relevant levels," *Sci. Total Environ.*, vol. 216, no. 11, p. 137095, 2020.
4. H. M. Chopade and H. B. Mathews, "Disposition and metabolism of 2-bromo-4,6-dinitroaniline in the male F344 rat," *Drug Metab. Dispos.*, vol. 17, no. 1, pp. 37–50, 1986.
5. R. Paliwal, R. Malik, and R. Kant, "Voltammetric behavior of 2-bromo-4,6-dinitroaniline in aqueous medium," *J. Electroanal. Chem.*, vol. 847, no. 6, p. 113375, 2019.
6. Y. Wang, H. Wang, and H. Xie, "Zero-valent iron effectively enhances valuable products generated by wastewater containing 2-bromo-4,6-dinitroaniline using hydrolysis acidification process," *J. Hazard. Mater.*, vol. 445, no. 3, p. 130515, 2023.
7. P. M. Kramer, S. Forester, and E. Kremmer, "Enzyme-linked immunosorbent assays for the sensitive analysis of 2,4-dinitroaniline and 2,6-dinitroaniline in water and soil," *Anal. Bioanal. Chem.*, vol. 391, no. 5, pp. 1821–1835, 2008.
8. A. Kawai, S. Goto, Y. Matsumoto, and H. Matsushita, "Mutagenicity of aliphatic and aromatic nitro compounds. Industrial, materials and related compounds," *Jpn. J. Ind. Health*, vol. 29, no. 1, pp. 34–54, 1987.
9. E. J. Weber, "Degradation of disperse blue 79 in anaerobic sediment-water systems," *Environ. Toxicol. Chem., USA*, 1988.
10. R. J. Tkacz and R. J. Maguire, "Occurrence of dyes in the Yamaska River, Quebec," *Water Qual. Res. J. Can.*, vol. 26, no. 2, pp. 145–162, 1991.
11. X. Zhou, Y. Zhou, J. Liu, S. Song, J. Sun, G. Zhu, H. Gong, L. Wang, C. Wu, and M. Li, "Study on the pollution characteristics and emission factors of PCDD/Fs from disperse dye production in China," *Chemosphere*, vol. 228, no. 8, pp. 328–334, 2019.
12. C. Niessner and U. Becker-Ross, "Detection of bromine in thermoplasts from consumer electronics by laser-induced plasma spectroscopy," *At. Spectrosc.*, vol. 59, no. 3, pp. 335–343, 2004.
13. S. J. Sondheimer, N. J. Bunce, M. E. Lemke, and C. A. Fyfe, "Acidity and catalytic activity of Nafion-H," *Macromolecules*, vol. 19, no. 2, pp. 339–343, 1986.
14. A. T. Peters and H. S. Freeman, "Physico-chemical Principles of Color Chemistry", Berlin, Germany: Springer Nature, 1996.